Collective-Mode Enhanced Matter-Wave Optics

Christian Deppner, Waldemar Herr, Merle Cornelius, Peter Stromberger, Tammo Sternke, Christoph Grzeschik, Alexander Grote, Jan Rudolph, Sven Herrmann, Markus Krutzik, et al.

Collective-mode enhanced matter-wave optics

Christian Deppner,[1] Waldemar Herr,[1,2] Merle Cornelius,[3] Peter Stromberger,[4] Tammo Sternke,[3] Christoph Grzeschik,[5] Alexander Grote,[4] Jan Rudolph,[1,*] Sven Herrmann,[3] Markus Krutzik,[5] André Wenzlawski,[4] Robin Corgier,[1,6,†] Eric Charron,[6] David Guéry-Odelin,[7] Naceur Gaaloul,[1] Claus Lämmerzahl,[3] Achim Peters,[5] Patrick Windpassinger,[4] and Ernst M. Rasel[1,‡]

[1] *Institut für Quantenoptik, Leibniz Universität Hannover, Welfengarten 1, D-30167 Hannover, Germany*
[2] *Deutsches Zentrum für Luft- und Raumfahrt e.V. (DLR), Institut für Satellitengeodäsie und Inertialsensorik, c/o Leibniz Universität Hannover, DLR-SI, Callinstr. 36, D-30167 Hannover, Germany*
[3] *ZARM, Universität Bremen, Am Fallturm 2, D-28359 Bremen, Germany*
[4] *Johannes Gutenberg-Universität Mainz, Staudingerweg 7, D-55128 Mainz, Germany*
[5] *Institut für Physik, Humboldt-Universität zu Berlin, Newtonstraße 15, D-12489 Berlin, Germany*
[6] *Université Paris-Saclay, CNRS, Institut des Sciences Moléculaires d'Orsay, F-91405 Orsay, France*
[7] *Laboratoire de Collisions Agrégats Réactivité (LCAR), CNRS, IRSAMC, Université de Toulouse, 118 Route de Narbonne, F-31062 Toulouse, France*

(Dated: March 11, 2021)

In contrast to light, matter-wave optics of quantum gases deals with interactions even in free space and for ensembles comprising millions of atoms. We exploit these interactions in a degenerate quantum gas as an adjustable lens for coherent atom optics. By combining a quadrupole-mode excitation of a Bose-Einstein Condensate (BEC) with a magnetic lens, we form a time-domain matter-wave lens-system. The focus is tuned by the strength of the lensing potential and the oscillatory phase of the quadrupole-mode. By placing the focus at infinity, we lower the total internal kinetic energy of a BEC comprising 101(37) k atoms in three dimensions to $^3/_2\ k_B \cdot 38^{+6}_{-7}$ pK. Our method paves the way for free-fall experiments lasting ten or more seconds as envisioned for tests of fundamental physics and high-precision BEC interferometry as well as opens up a new kinetic energy regime.

Optics with matter-waves shares many analogies with its counterpart for light. However, matter can interact via electromagnetic forces, a well known fact in electron or ion optics, where the Coulomb repulsion causes particle beams to diverge, deteriorating their quality [1]. Similarly, interactions accelerate the expansion of a repulsive quantum gas in free-fall and, moreover, become dominant at ultra-low temperatures, setting a lower limit to the internal kinetic energy of the gas [2].

So far, evaporative cooling [3] and spin gradient cooling [4] permitted to reach three-dimensional internal kinetic energies below 500 pK and 350 pK, respectively. In terms of effective temperatures, employing matter-wave lenses based on magnetic [5–7], electrostatic [8] or optical [9] forces made it possible to reduce the internal kinetic energy of a BEC to about 50 pK [10], albeit only in two dimensions.

We tailor the expansion of a ^{87}Rb BEC by exploiting a collective-mode excitation in the BEC [11, 12] in combination with a magnetic lens. Both act together like a time-domain matter-wave lens-system for all three spatial dimensions. The focus of the lens-system can be tuned by releasing the BEC at an appropriate phase of the collective-mode oscillation and the strength of the lensing potential. When focusing at infinity, we achieve a total internal kinetic energy in three dimensions of as low as $^3/_2\ k_B \cdot 38^{+6}_{-7}$ pK.

Such atomic ensembles allow for placing better experimental constraints on proposed modifications of quantum theory [13–15]. Moreover, they fulfill the strict requirements concerning the atomic expansion for experiments, where BECs fall freely during tens of seconds in an atom interferometer [16–18] as needed e. g. for a stringent quantum test of the equivalence principle [19–21], gravitational wave detection [22, 23] or the determination of the gravitational constant [24] and the photon recoil [25].

Our matter-wave lens-system is implemented using an atom-chip (Fig. 1a), which permits to excite the BEC to perform collective-mode oscillations (Fig. 1b), to release it at a specific phase and to shape it with a magnetic lens. Fig. 1c - Fig. 1e compares simulated absorption images of a BEC obtained with and without our method. The release of the BEC at a phase φ of the oscillation, where it expands in all three directions (red arrows) without and with applying a magnetic lens (green arrows) leading to delta-kick collimation (DKC) in Fig. 1c and Fig. 1d, serves as a reference for our experiments. Without the magnetic lens, we achieve an internal kinetic energy of $^3/_2\ k_B \cdot 2$ nK. The atom-chip based magnetic lens, which typically has a cylindrical shape, can lower the expansion rate mainly along the radial direction, resulting in a total energy of $^3/_2\ k_B \cdot 167$ pK. Exploiting the quadrupole-mode (QM) oscillation, we lower the BEC's expansion along the axial direction, where the magnetic lens lacks refractive power. By tailoring the highly anisotropic expansion to the magnetic lens, our time-domain lens-system resulted in an internal kinetic energy of $^3/_2\ k_B \cdot 38$ pK, as shown in Fig. 1e.

The experiments, using the high-flux BEC source detailed in [26], were conducted in the Bremen Drop Tower,

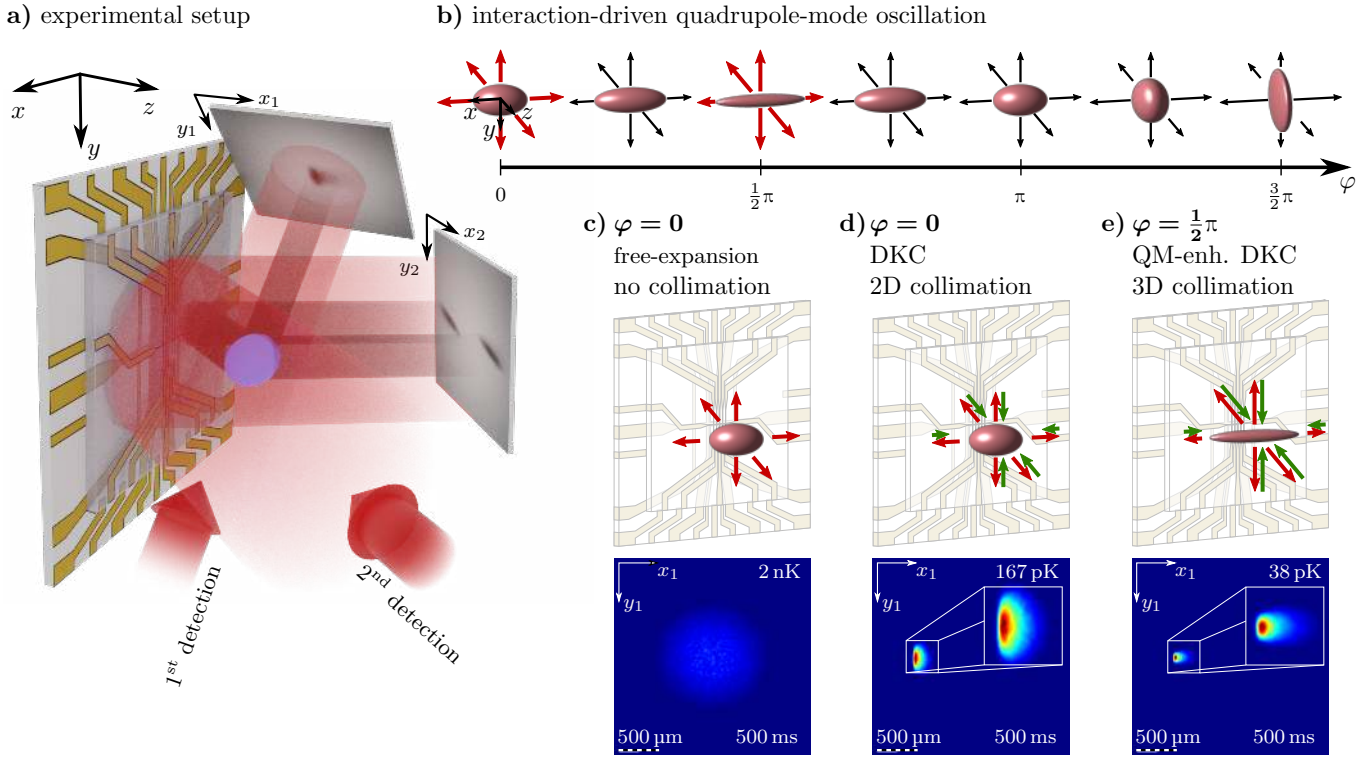

FIG. 1. Interaction based time-domain matter-wave lens-system. The BEC, created on an atom-chip, is released and is then either freely drifting, or is briefly exposed to a magnetic lensing potential. Absorption images from two different directions provide full 3D information of the BEC's position and spatial distribution, as shown in a). Before its release, the BEC is excited to perform a quadrupole-mode oscillation as depicted in b). Depending on its phase φ, the size and expansion of the BEC varies. In c), the BEC freely expands in all directions with an internal kinetic energy of $^3/_2\, k_B \cdot 2\,\mathrm{nK}$. In d), the green arrows depict the effect of a cylindrical magnetic lens, reducing U_{kin} to $^3/_2\, k_B \cdot 167\,\mathrm{pK}$. Choosing the release at an oscillatory phase, such that the BEC is only weakly expanding in axial direction, allows in combination with the effect of the cylindrical magnetic lens to reach the lowest energy of $^3/_2\, k_B \cdot 38\,\mathrm{pK}$, shown in e).

providing a free-fall lasting for 4.74 s. During the drops, BECs of about 100 k atoms were created in a cylindrically shaped Ioffe-Pritchard trap [27, 28] with final evaporation-trap frequencies of $f_{\mathrm{evap}} = \{24, 457, 462\}$ Hz along the x-, y- and z-direction, respectively. Before the release, we excite a quadrupole-mode oscillation in the BEC [11, 12] by swiftly reducing the magnetic bias-field in x-direction within 0.5 ms, increasing only the strong trap frequencies to $f_{\mathrm{QM}} = \{24, 550, 554\}$ Hz. After a delay of 0.4 ms, accounting for a magnetic field settling time, the BEC is transported along the z-direction within 150 ms to its release position 1462 µm away from the atom-chip by reducing the magnetic bias-field in the y-direction. During this transport, the trap frequencies reduce to $f_{\mathrm{release}} = \{9.1, 27.9, 24.6\}$ Hz. A shortcut-to-adiabaticity protocol is used to minimize the amplitude of a residual center-of-mass dipole oscillation of the BEC to $A_{\mathrm{release}} = \{1.20(59), 0.30(12), 4.00(19)\}$ µm [29].

During the free expansion after release, the BEC's internal interaction energy is converted into kinetic energy. After 80 ms, the expansion reaches a ballistic regime and a three-dimensional, predominantly cylindrical magnetic lens is applied. Close to the center, the lens potential along the x- and y-axis is well described by the harmonic approximation with potential frequencies of $\omega_x = 2\pi \cdot 2.9\,\mathrm{rad/s}$ and $\omega_y = 2\pi \cdot 10.6\,\mathrm{rad/s}$. However, along the z-axis, the potential deviates from a simple harmonic shape at larger distances to the center and can be approximated by $V_z = 1/2 m\omega_z^2 z^2(1 + z/L3 + z^2/L4^2)$, with $\omega_z = 2\pi \cdot 10.6\,\mathrm{rad/s}$, $L3 = 1225\,\mu\mathrm{m}$ and $L4 = 2933\,\mu\mathrm{m}$. After a 2.42 ms exposure to the lens, a subsequent RF-driven adiabatic-rapid-passage [30] transfers 87.1(2) % of the atoms from the state $|F = 2, m_F = 2\rangle$ into the $|F = 2, m_F = 0\rangle$ in order to reduce their susceptibility to residual magnetic fields [31].

Absorption images [32] from one of the two directions available taken at different times (Fig. 1a) provide complete information about motion and expansion of the BEC over time. Without applying our time-domain lens-system, BECs were imaged up to 160 ms after release. With our lens-system we could stretch this time to 2 s. To record this data, we performed 56 BEC experiments over a time of ten weeks, consuming 34 drops in the Bre-

men Drop Tower. Despite this limited number of drops, the data is sufficient to gauge our simulation of the experiment and to optimize our matter-wave lens-system.

Lowering the internal kinetic energy of the released BEC requires a careful adjustment of the lens-system and, hence, an analysis of the quadrupole-mode. For this purpose, we determined the aspect-ratios of the Thomas-Fermi radii(R) by absorption imaging for varying hold-times of the BEC in the release trap. In Fig. 2, the measured aspect-ratios, defined by R_{x_1}/R_{y_1} (blue) and R_{x_2}/R_{y_2} (orange), are shown together with the results of a 3D collective-mode simulation of the BEC in the magnetic trap (solid lines) based on a variational approach [33, 34]. A damping-time of 300 ms was introduced in our simulation, to consider residual thermal atoms in the trap [35, 36], as well as the anharmonicities of the lens potential [37]. With these additions, the simulation is in good agreement with the measured data. The Fourier transform of the shape-oscillation shows a large amplitude of the quadrupole-mode with a small admixture of a monopole-mode.

A hold-time of 18.46 ms (dashed line in Fig. 2) turned out to be optimal for our purpose as the BEC has already passed the turning point of the quadrupole-mode oscillation along the x-direction. The collapse along the weak axis counteracts the emerging accelerating expansion due to the interaction energy, improving the collimation along this axis. This hold-time coincides with the turning point of the dipole oscillation in z-direction, reducing the center-of-mass velocity of the BEC in total to $v_{xyz} = \{56(26), -56(69), 139(17)\}$ µm/s.

Fig. 3 summarizes the experimental results (colored diamonds) as well as the numerical simulation (colored lines) of tailoring the expansion of the BEC with our time-domain lens-system by focussing the matter-wave at infinity in 3D. For comparison, the effect of the oscillation without magnetic lens (circles) as well as numerical simulations of employing only a magnetic lens for collimation (dashed colored lines) are shown.

The root of the second moments of the one-dimensional density distribution serves as a measure of the BEC's size. This is motivated by the shapes of the BECs observed after evolution times of several hundreds of milliseconds. Here, a more and more pronounced tail appears in the density distribution, pointing in z-direction, which stems from the anharmonicity of the magnetic lens. Therefore, the shape of the BEC along this direction cannot be characterized by a Thomas-Fermi fit and a simple harmonic scaling-approach [38] is not sufficient to describe its evolution.

In order to obtain numerical pictures, we model the spatial density and corresponding velocity distribution of the BEC after a free expansion of 80 ms. The effect of the lens and the free evolution until detection is calculated based on a three-dimensional interaction-free particle-simulation, where the atoms as classical particles

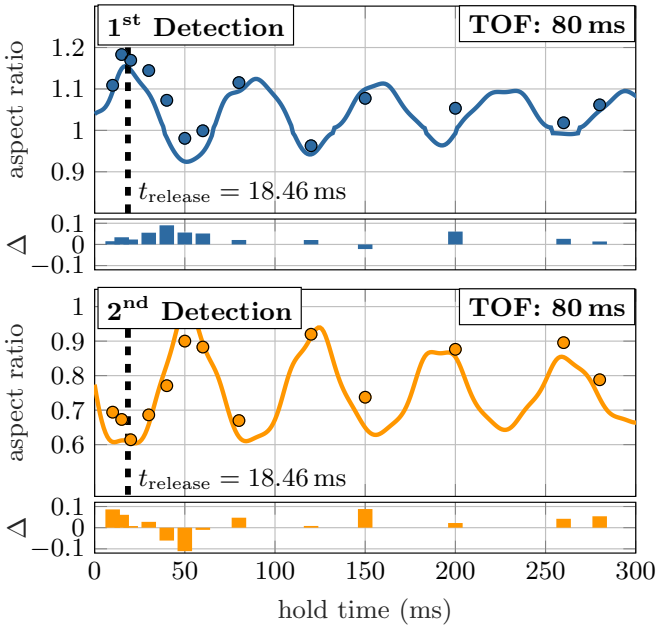

FIG. 2. Collective-mode oscillation of the BEC in the release trap as observed after 80 ms time-of-flight. The aspect-ratio in dependence of the hold-time in the release trap derived from both detection systems (circles) is shown next to our simulation (lines). The bar graphs show their residuals to the simulation. The dashed lines indicate the instance of release where our time-domain lens-system is optimally collimating the BEC.

are stochastically sampled from a classical probability distribution that gives the correct position and momentum densities. From the spatial densities, absorption images for all directions of observation are computed. To fit the numerical images to the experimental data, the pixel-wise difference is computed and minimized at once using a non-linear least-squares algorithm. Free fit-parameters are global corrections to the initial spatial and velocity distribution, the effective duration of the applied lens, accounting for a non-instantaneous switching, as well as a rotation and position offset of the lens potential relative to the BEC. Furthermore, the efficiency of the adiabatic-rapid-passage of 87.1(2) % is taken into account. Shot-to-shot atom fluctuation and frequency instability of the detection laser, which affect each data-point individually, required additional correction parameters to be added.

From the fit, all relevant properties, especially the velocity distribution can be obtained. As a cross-check, a particle number of 101(37) k atoms was fitted, which is in good agreement with the particle number of 98(38) k atoms extracted from five experiments, where a BEC is simply released from the trap and imaged after 80 ms of free evolution. The spread in particle number arises due to day-to-day fluctuations of the system's performance and has the largest influence on the BEC's expansion and, by this, on the uncertainty of the total internal kinetic energy. The combined uncertainties of the other

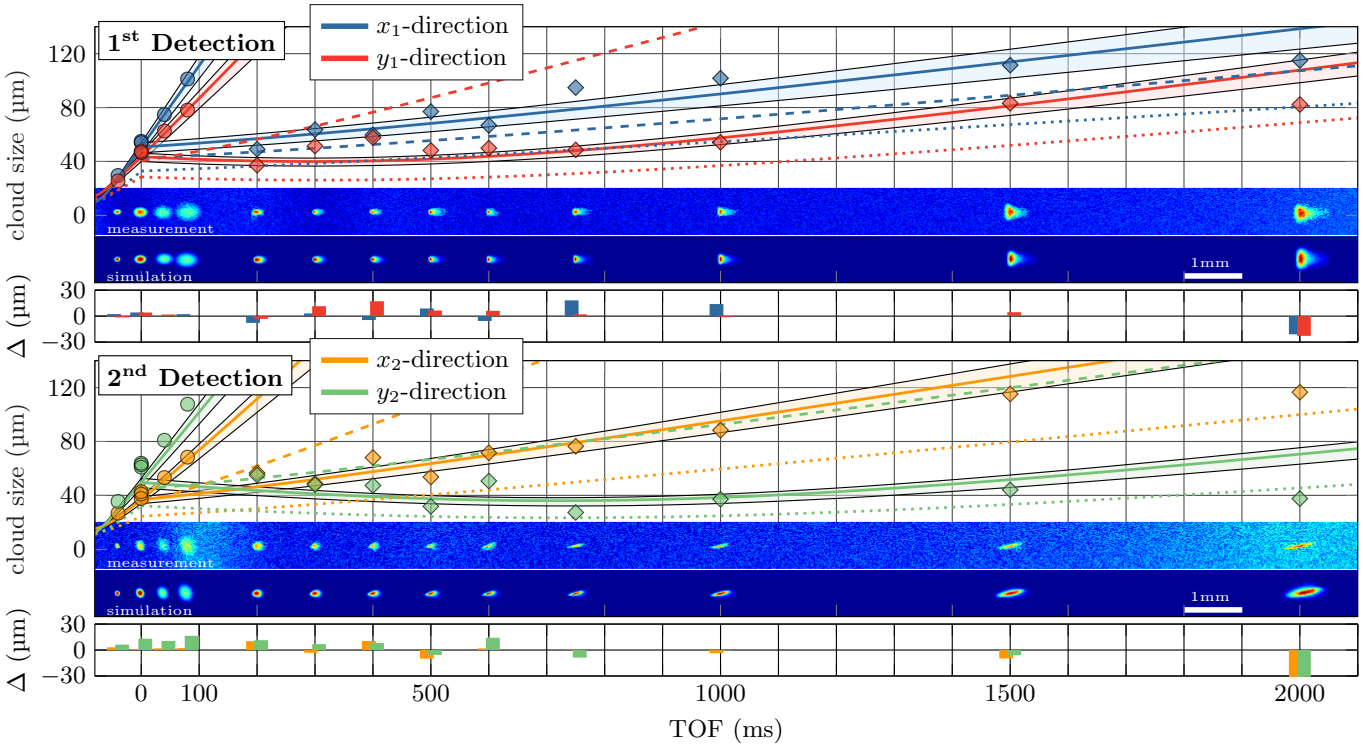

FIG. 3. Free evolution of a BEC collimated with our time-domain lens-system. As a measure of size, the root of the one-dimensional second moments of the absorption images' spatial distribution depicted underneath the respective graphs is shown. The results obtained employing only the quadrupole-mode oscillation (circles, compare Table I "free exp.") and the impact of the time-domain lens-system (diamonds, compare Table I "QM-enh. DKC") is shown next to our 3D particle-simulation (colored lines) fitted to the experimental data. The bar graphs represent their residuals to the 3D particle-simulation. The shaded areas reflect the uncertainty in the particle number. The BECs featured typically 101(37) k atoms and an internal kinetic energy of $^3/_2\ k_B \cdot 38^{+6}_{-7}$ pK after the application of our time-domain lens-system. Our simulation allows us to compare our method with delta-kick collimation only, which results in a significantly larger expansion rate (dashed lines, compare Table I "DKC"). Additionally, the dotted lines compare the simulated expansion of a BEC with 10 k atoms displaying a lower mean-field energy, corresponding to $U_{\mathrm{kin}} = {}^3/_2\ k_B \cdot 14\,\mathrm{pK}$.

fit parameters contribute on the order of less than one picokelvin and are therefore negligible.

From the numerical images, the expansion of the BEC (colored lines) and the fit-uncertainties (shaded areas) were computed. The time-domain lens-system reduces the total internal kinetic energy of the initial BECs, amounting to $^3/_2\ k_B \cdot 2\,\mathrm{nK}$, to $^3/_2\ k_B \cdot 38^{+6}_{-7}\,\mathrm{pK}$, corresponding to an expansion velocity of as low as $\sigma_v = \{77^{+7}_{-5}, 47^{+4}_{-3}, 53^{+7}_{-6}\}$ µm/s. The combined action of quadrupole-mode oscillation and delta-kick collimation favorably compares to the case, where solely delta-kick collimation is applied (dashed lines), leading to $U_{\mathrm{kin}} = {}^3/_2\ k_B \cdot 167\,\mathrm{pK}$. Table I confronts the internal kinetic energies in all three directions obtained with the different methods.

The minimal achievable internal kinetic energy is determined by the residual interaction energy of the BEC after the magnetic lens and amounts to $^3/_2\ k_B \cdot 26\,\mathrm{pK}$. Ideally, further reduction of U_{kin} could be achieved by extending the time of free expansion prior to the magnetic lens, but the anharmonicities of the latter would hinder reaching even lower expansion rates in our current setup. To mitigate this lens abberation one could form a more complex multi-lens system in analogy to light-optics.

TABLE I. 1D and 3D internal kinetic energy of the BEC during free expansion and after DKC with and without quadrupole-mode enhancement. The residual interaction energy of the BEC constitutes the limit for the lowest achievable kinetic energy in this setup.

dimension	free exp.	DKC	QM-enh. DKC	limit
$U_{\mathrm{kin,x}}/\,(^1/_2\ k_B)$	659 pK	447 pK	62^{+8}_{-11} pK	45 pK
$U_{\mathrm{kin,y}}/\,(^1/_2\ k_B)$	3020 pK	36 pK	24^{+3}_{-4} pK	17 pK
$U_{\mathrm{kin,z}}/\,(^1/_2\ k_B)$	2658 pK	16 pK	29^{+6}_{-7} pK	16 pK
$U_{\mathrm{kin}}/\,(^3/_2\ k_B)$	2112 pK	167 pK	38^{+6}_{-7} pK	26 pK

Even slower expansion could also be achieved by simply reducing the number of atoms. For reference, the dotted lines in Fig. 3 show the simulated expansion of a BEC with only 10 k atoms, leading to $U_{\mathrm{kin}} = {}^3/_2\ k_B \cdot 14\,\mathrm{pK}$.

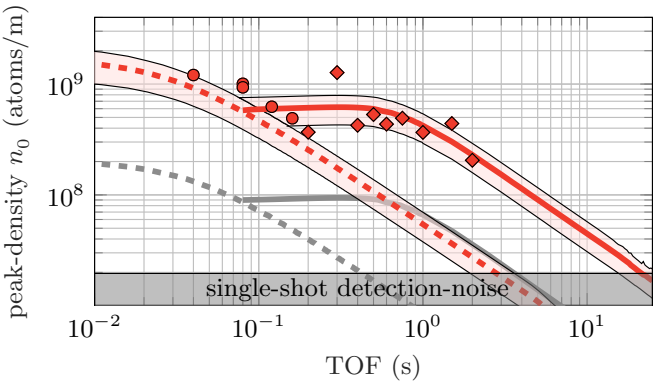

FIG. 4. Detectability of a BEC using our matter-wave lens-system in dependence of the time-of-flight without (with) employing our time-domain lens-system depicted as circles (diamonds). The peak-density along the y_1 direction of the twice integrated simulated BEC's spatial density distribution is compared with the data and the noise of our imaging system. Our freely evolving BEC with 101(37) k atoms at $^3/_2\ k_B \cdot 2\,\mathrm{nK}$ (dashed red line) is visible for approximately 2.25 s, which is greatly extended to 17 s by reducing U_{kin} to $^3/_2\ k_B \cdot 38^{+6}_{-7}\,\mathrm{pK}$ using our lens-system (solid red line). The shaded area reflects the uncertainty in the atom number. The gray lines show the same simulation, but with a BEC composed of 10 k atoms leading to a much shorter detectability of 3.5 s, although the internal kinetic energy would be at $^3/_2\ k_B \cdot 14\,\mathrm{pK}$.

However, the BEC's detectability over time decreases drastically with the atom number.

Our method allows us to largely extend the free evolution time of the BEC before it becomes too dilute to be detected by absorption imaging. Here, we define this time to be the moment the absorption signal of the BEC's peak-density approaches the single-shot detection-noise, obtained from the background-noise in the absorption images.

The peak-density has been simulated for a BEC shaped by our matter-wave lens-system and for a simple release. While in the latter case, the BEC is visible until approximately 2.25 s, our method extends this time to 17 s, as shown in Fig. 4. The gray line, in comparison, represents the detectability of a BEC with only 10 k atoms at $U_{\mathrm{kin}} = {}^3/_2\ k_B \cdot 14\,\mathrm{pK}$ that, even if the internal kinetic energy is lower, is only visible for 3.5 s.

In conclusion, interactions that are often compromising matter-wave optics, were exploited using collective-mode excitations of a BEC for shaping its evolution. In combination with a magnetic lens, we realized a time-domain lens-system with a focus adjustable by the oscillatory phase at the condensate's release and the strength of the lensing potential. Focusing at infinity, we reduced the free expansion of a BEC in all three dimensions, yielding unprecedentedly low internal kinetic energies of $^3/_2\ k_B \cdot 38^{+6}_{-7}\,\mathrm{pK}$. In this way, we sampled the time evolution of BECs comprising 101(37) k atoms for up to two seconds during free-fall in the Bremen Drop Tower.

According to our simulations, these slowly expanding BECs would be detectable by absorption imaging even after 17 s, exceeding by far the microgravity time offered by the Drop Tower. They represent an exceptional input state for atom interferometry lasting for ultra-long time-scales. Next to high precision atom interferometric tests, we anticipate that our method will be important for e. g. shaping a BEC to analyse the wave-fronts of light fields and to estimate their possible biases in light-pulse atom interferometers [39].

Obviously, our method can also be employed with attractive or tunable interactions [40] and diverging magnetic lenses [41, 42]. Interactions are nowadays also exploited to establish non-classical correlations. Our method might be of interest in this context. Delta-kicks start to be explored in squeezing experiments [43, 44] and can be an interesting addition to other squeezing schemes [45]. Furthermore, such spin-polarized, dilute and slowly expanding gases are important for metrology [46, 47] as well as quantum gas experiments in drop towers [7, 26], fountains [10] and space, as envisioned by the ISS space mission BECCAL [48].

We acknowledge valuable discussions with R. Walser. This work is supported by the German Space Agency (DLR) with funds provided by the Federal Ministry for Economic Affairs and Energy (BMWi) due to an enactment of the German Bundestag under Grant No. DLR 50WM1552-1557 (QUANTUS-IV Fallturm), as well as by the Centre for Quantum Engineering and Space-Time Research (QUEST).

* Current address: Department of Physics, Stanford University, Stanford, California 94305, USA
† Current address: Quantum Science and Technology Arcetri INO-CNR, Largo Enrico Fermi 2, I-50125 Firenze, Italy
‡ To whom correspondence should be addressed. rasel@iqo.uni-hannover.de

[1] G. Jansen, Nuclear Instruments and Methods in Physics Research Section A: Accelerators, Spectrometers, Detectors and Associated Equipment **298**, 496 (1990).
[2] W. Ketterle, D. S. Durfee, and D. M. Stamper-Kurn, (1999), arXiv:cond-mat/9904034 [cond-mat].
[3] A. E. Leanhardt, T. A. Pasquini, M. Saba, A. Schirotzek, Y. Shin, D. Kielpinski, D. E. Pritchard, and W. Ketterle, Science **301**, 1513 (2003), https://science.sciencemag.org/content/301/5639/1513.full.pdf.
[4] P. Medley, D. M. Weld, H. Miyake, D. E. Pritchard, and W. Ketterle, Phys. Rev. Lett. **106**, 195301 (2011).
[5] H. Friedburg, Zeitschrift für Physik **130**, 493 (1951).
[6] H. Ammann and N. Christensen, Phys. Rev. Lett. **78**, 2088 (1997).
[7] H. Müntinga, H. Ahlers, M. Krutzik, A. Wenzlawski, S. Arnold, D. Becker, *et al.*, Phys. Rev. Lett. **110**, 093602 (2013).

[8] J. G. Kalnins, J. M. Amini, and H. Gould, Physical Review A **72**, 043406 (2005).

[9] S. Chu, J. Bjorkholm, A. Ashkin, J. Gordon, and L. Hollberg, Optics letters **11**, 73 (1986).

[10] T. Kovachy, J. M. Hogan, A. Sugarbaker, S. M. Dickerson, C. A. Donnelly, C. Overstreet, and M. A. Kasevich, Phys. Rev. Lett. **114**, 143004 (2015).

[11] D. S. Jin, J. R. Ensher, M. R. Matthews, C. E. Wieman, and E. A. Cornell, Phys. Rev. Lett. **77**, 420 (1996).

[12] M.-O. Mewes, M. R. Andrews, N. J. van Druten, D. M. Kurn, D. S. Durfee, C. G. Townsend, and W. Ketterle, Phys. Rev. Lett. **77**, 988 (1996).

[13] A. Bassi, K. Lochan, S. Satin, T. P. Singh, and H. Ulbricht, Reviews of Modern Physics **85**, 471 (2013).

[14] S. Nimmrichter and K. Hornberger, Phys. Rev. Lett. **110**, 160403 (2013).

[15] S. Vowe, C. Lämmerzahl, and M. Krutzik, Phys. Rev. A **101**, 043617 (2020).

[16] S. S. Szigeti, J. E. Debs, J. J. Hope, N. P. Robins, and J. D. Close, New Journal of Physics **14**, 023009 (2012).

[17] S. Abend, M. Gebbe, M. Gersemann, H. Ahlers, H. Müntinga, E. Giese, *et al.*, Phys. Rev. Lett. **117**, 203003 (2016).

[18] H. Ahlers, H. Müntinga, A. Wenzlawski, M. Krutzik, G. Tackmann, S. Abend, *et al.*, Phys. Rev. Lett. **116**, 173601 (2016).

[19] T. Schuldt, C. Schubert, M. Krutzik, L. G. Bote, N. Gaaloul, J. Hartwig, *et al.*, Experimental Astronomy **39**, 167 (2015).

[20] D. N. Aguilera, H. Ahlers, B. Battelier, A. Bawamia, A. Bertoldi, R. Bondarescu, *et al.*, Classical and Quantum Gravity **31**, 115010 (2014).

[21] J. Williams, S.-w. Chiow, N. Yu, and H. Müller, New Journal of Physics **18**, 025018 (2016).

[22] J. M. Hogan, D. M. Johnson, S. Dickerson, T. Kovachy, A. Sugarbaker, S.-w. Chiow, *et al.*, General Relativity and Gravitation **43**, 1953 (2011).

[23] P. W. Graham, J. M. Hogan, M. A. Kasevich, and S. Rajendran, Physical review letters **110**, 171102 (2013).

[24] G. Rosi, F. Sorrentino, L. Cacciapuoti, M. Prevedelli, and G. Tino, Nature **510**, 518 (2014).

[25] D. S. Weiss, B. C. Young, and S. Chu, Physical review letters **70**, 2706 (1993).

[26] J. Rudolph, W. Herr, C. Grzeschik, T. Sternke, A. Grote, M. Popp, D. Becker, H. Müntinga, H. Ahlers, and A. Peters, New J. Phys. **17**, 065001 (2015).

[27] Y. T. Baiborodov, M. S. Ioffe, V. M. Petrov, and R. I. Sobolev, Journal of Nuclear Energy. Part C, Plasma Physics, Accelerators, Thermonuclear Research **5**, 409 (1963).

[28] D. E. Pritchard, Phys. Rev. Lett. **51**, 1336 (1983).

[29] R. Corgier, S. Amri, W. Herr, H. Ahlers, J. Rudolph, D. Guéry-Odelin, E. M. Rasel, E. Charron, and N. Gaaloul, New Journal of Physics **20**, 055002 (2018).

[30] M. Loy, Phys. Rev. Lett. **32**, 814 (1974).

[31] T. van Zoest, N. Gaaloul, Y. Singh, H. Ahlers, W. Herr, S. T. Seidel, *et al.*, Science **328**, 1540 (2010).

[32] G. Reinaudi, T. Lahaye, Z. Wang, and D. Guéry-Odelin, Opt. Lett. **32**, 3143 (2007).

[33] V. M. Perez-Garcia, H. Michinel, J. Cirac, M. Lewenstein, and P. Zoller, Physical review letters **77**, 5320 (1996).

[34] V. M. Perez-Garcia, H. Michinel, J. Cirac, M. Lewenstein, and P. Zoller, Physical Review A **56**, 1424 (1997).

[35] D. M. Stamper-Kurn, H.-J. Miesner, S. Inouye, M. R. Andrews, and W. Ketterle, Phys. Rev. Lett. **81**, 500 (1998).

[36] D. Guéry-Odelin and S. Stringari, Phys. Rev. Lett. **83**, 4452 (1999).

[37] G. Bismut, B. Pasquiou, E. Maréchal, P. Pedri, L. Vernac, O. Gorceix, and B. Laburthe-Tolra, Phys. Rev. Lett. **105**, 040404 (2010).

[38] Y. Castin and R. Dum, Physical Review Letters **77**, 5315 (1996).

[39] R. Karcher, A. Imanaliev, S. Merlet, and F. P. Dos Santos, New Journal of Physics **20**, 113041 (2018).

[40] R. Corgier, S. Loriani, H. Ahlers, K. Posso-Trujillo, C. Schubert, E. M. Rasel, E. Charron, and N. Gaaloul, New Journal of Physics **22**, 123008 (2020).

[41] J. P. D'Incao, M. Krutzik, E. Elliott, and J. R. Williams, Physical Review A **95**, 012701 (2017).

[42] S. Y. Van De Meerakker, H. L. Bethlem, and G. Meijer, Nature Physics **4**, 595 (2008).

[43] F. Anders, A. Idel, P. Feldmann, D. Bondarenko, S. Loriani, K. Lange, J. Peise, M. Gersemann, B. Meyer, S. Abend, *et al.*, arXiv preprint arXiv:2010.15796 (2020).

[44] Y. Wu, R. Krishnakumar, J. Martínez-Rincón, B. K. Malia, O. Hosten, and M. A. Kasevich, Physical Review A **102**, 012224 (2020).

[45] S. S. Szigeti, S. P. Nolan, J. D. Close, and S. A. Haine, Physical Review Letters **125**, 100402 (2020).

[46] P. Asenbaum, C. Overstreet, T. Kovachy, D. D. Brown, J. M. Hogan, and M. A. Kasevich, Phys. Rev. Lett. **118**, 183602 (2017).

[47] P. Asenbaum, C. Overstreet, M. Kim, J. Curti, and M. A. Kasevich, (2020), arXiv:2005.11624 [physics.atom-ph].

[48] K. Frye, S. Abend, W. Bartosch, A. Bawamia, D. Becker, H. Blume, *et al.*, (2019), arXiv:1912.04849 [physics.atom-ph].